

# Fractional $\hbar$ -scaling for quantum kicked rotors without cantori

J. Wang,<sup>1,2</sup> T.S. Monteiro,<sup>3,\*</sup> S. Fishman,<sup>4</sup> and J.P. Keating and R. Schubert<sup>5</sup>

<sup>1</sup>*Temasek Laboratories, National University of Singapore, 117542 Singapore.*

<sup>2</sup>*Beijing-Hong Kong-Singapore Joint Center for Nonlinear and Complex Systems (Singapore), National University of Singapore, 117542 Singapore.*

<sup>3</sup>*Department of Physics and Astronomy, University College London, Gower Street, London, United Kingdom, WC1E 6BT*

<sup>4</sup>*Physics Department, Technion, Haifa, IL-32000, Israel*

<sup>5</sup>*School of Mathematics, University of Bristol, Bristol BS8 1TW, U.K.*

(Dated: February 2, 2018)

Previous studies of quantum delta-kicked rotors have found momentum probability distributions with a typical width (localization length  $L$ ) characterized by fractional  $\hbar$ -scaling, ie  $L \sim \hbar^{2/3}$  in regimes and phase-space regions close to ‘golden-ratio’ cantori. In contrast, in typical chaotic regimes, the scaling is integer,  $L \sim \hbar^{-1}$ . Here we consider a generic variant of the kicked rotor, the random-pair-kicked particle (RP-KP), obtained by randomizing the phases every second kick; it has no KAM mixed phase-space structures, like golden-ratio cantori, at all. Our unexpected finding is that, over comparable phase-space regions, it also has fractional scaling, but  $L \sim \hbar^{-2/3}$ . A semiclassical analysis indicates that the  $\hbar^{2/3}$  scaling here is of quantum origin and is not a signature of classical cantori.

PACS numbers: 05.45.Mt, 32.80.Pj

A notable recent achievement of atom optics has been the realization of a well-known paradigm of quantum chaos, the quantum ‘ $\delta$ -kicked particle’ (DKP) [1, 2]. Laser-cooled atoms in a pulsed periodic optical potential can be effectively modeled theoretically by the Hamiltonian  $H = p^2/2 - k \cos x \sum_n \delta(t - nT)$  provided the pulses are sufficiently short. This system has been extensively investigated in numerous theoretical (see eg [3, 4]) and experimental [5] studies by several groups worldwide. In the chaotic regime ( $kT \gg 1$ ) the momentum distributions  $N(p, t)$  evolve into a final, time-independent distribution of exponential form:  $N(p, t \rightarrow \infty) \sim \exp(-|p|/L)$ .  $L$ , the momentum localization length, has well-known integer scaling properties  $L \sim K^2 \hbar^{-1}$ . This effect, termed ‘dynamical localization (DL)’, has been well-studied both experimentally and theoretically.

But an important exception, with  $L \sim \hbar^{2/3}$ , was found in the seminal theoretical study of quantum behavior in the vicinity of so-called ‘golden-cantori’ in [6]. At a critical value of  $kT \approx 0.97$ , the last classical barrier (KAM torus) which impedes chaotic diffusion is broken. What remains are fractal partial barriers, termed cantori, situated at momenta  $p \approx 2\pi R$  and  $p \approx 2\pi(R - 1)$ , (or integer multiples thereof) where  $R$  is the golden ratio. A subsequent study [7] suggested that a *positive* exponent  $L \sim \hbar^{+\sigma}$  was associated with tunnelling transport (favoured by increasing  $\hbar$ ) while a negative exponent  $L \sim \hbar^{-\sigma}$  was associated with dynamical localization where transport increases as  $\hbar \rightarrow 0$ . In [7] it was found that the sign of the scaling exponent can change from negative to positive as the dominant transport mechanism changes from tunnelling to dynamical localization. A study of the *classical* phase-space scaling near these golden tori [8] identified two characteristic scaling ex-

ponents,  $\sigma \approx 0.65$  and  $\sigma \approx 0.75$ . Since the fractional  $L \sim \hbar^\sigma \sim \hbar^{2/3}$  *quantum* scaling was found in regions close to  $p \sim 2\pi R$ , this behavior was attributed in [6] to the smaller of the classical exponents.

A recent study [10] of a closely related system, the double-kicked particle (2-DKP), found fractional scaling of momentum distributions with  $L \sim \hbar^{-0.75}$ , ie characterized by one of the classical golden ratio exponents - and in phase-space regions corresponding quite closely to those of [6]- it was argued that this too was evidence of the quantum signature of the golden cantori. As the 2-DKP has already been experimentally realized with cold atoms [9] and its fractional scaling occurs over a much broader range of  $p$  than for the usual DKP, this feature of the atomic momentum distributions is very amenable to experimental study.

However, here, we introduce a system which is random, but closely related to both the DKP and 2-DKP: the randomized-pair DKP or RP-DKP. It is obtained as a limit as the phases between consecutive kick-pairs become completely random. This system has no mixed phase-space regions or KAM cantori at all. This study, over a range of smaller  $\hbar$  values than [10] found the random system has exactly the same scaling properties as the mixed-phase-space 2-DKP. Both have  $L \sim \hbar^{-2/3}$  for small  $\hbar$ ; in [10] a slightly larger exponent was found because some non-asymptotic values of  $\hbar$  were included. This unexpected result is the key finding of our paper. A semiclassical analysis shows that the scaling with  $\hbar^{-2/3}$  arises naturally from the quantum unitary matrix and is not a signature of golden cantori. We discuss possible implications for the ordinary DKP.

The Hamiltonian of the 2-DKP is given by [10]  $H = \frac{P'^2}{2} - k \cos x \sum_N [\delta(t' - NT) + \delta(t' - NT + \epsilon)]$  where  $\epsilon \ll$

$T$  is a small time interval. In effect, the particles are exposed to a sequence of *pairs* of closely spaced  $\delta$ -kicks. One could now adopt the usual procedure and choose  $T$  to define the time unit and thence derive a classical map with a stochasticity parameter  $K = kT$  and momentum units  $p = P'T$ . However, we show below that, for the 2-DKP, it is the small timescale  $\epsilon$ , rather than the period  $T$ , which provides the natural unit of time. Hence, rescaling time as  $t'/\epsilon \rightarrow t$ , and  $P'\epsilon \rightarrow p$ , we obtain our 2-DKP map:

$$\begin{aligned} p_{N+1} &= p_N + K_\epsilon \sin x_N; & p_{N+2} &= p_{N+1} + K_\epsilon \sin x_{N+1} \\ x_{N+1} &= x_N + p_{N+1}; & x_{N+2} &= x_{N+1} + p_{N+2} \tau_\epsilon \end{aligned} \quad (1)$$

The classical stochasticity parameter  $K_\epsilon = k\epsilon$ . This map depends also on a further parameter  $\tau_\epsilon = (T - \epsilon)/\epsilon$ .

Clearly, we see that setting  $\tau_\epsilon = 1$  in Eq.(1) recovers the Standard Map or DKP. To obtain the 2-DKP, we take  $\tau_\epsilon \sim 10 - 100$ : typical experimental values used in [9] are  $\tau_\epsilon \approx 10 - 25$  and  $K_\epsilon = 0.1$  to  $0.5$ . The RP-DKP is obtained by taking the limit  $\tau_\epsilon \rightarrow \infty$ , causing the impulse  $\sin x_{N+2}$  to become randomized. This can be achieved in practice by keeping  $k$  and  $\epsilon$  constant and taking  $T \rightarrow \infty$ . In the usual  $T$ -scaled map this would yield an infinite stochasticity constant  $K = kT$  (but little insight). This RP-DKP limit has no mixed phase space behavior at all, but it retains the momentum trapping and its behavior is determined by the stochasticity parameter  $K_\epsilon$ . The map Eq.(1) has  $2\pi$  periodicity in these re-scaled momentum units for integer  $\tau_\epsilon$ .

Fig.1 (a) compares Poincaré surfaces of section (SOS) for the 2-DKP and RP-DKP. For the 2-DKP, a periodic structure of chaotic ‘cells’ separated by thin mixed-phase regions is apparent. These momentum ‘trapping’ regions appear at  $p \approx (2m+1)\pi$  where  $m = 0, \pm 1, \pm 2, \dots$ . For odd-integer multiples of  $\pi$  there is near-cancellation of consecutive kicks. Fig.1 (b) shows the RP-DKP, for which  $\tau_\epsilon = 10^6$ . In fact, an indistinguishable SOS can be obtained by taking actual random phases, i.e.  $x_{N+2} = 2\pi\zeta_N$  where  $0 < \zeta_N < 1$  is a random number chosen every kick pair. We see that the trapping is there, but with no trace of islands etc. The RP-DKP never has any islands, regardless of how small  $K_\epsilon$  becomes.

For the quantum equivalent we note that in a basis of plane waves, the one-period time-evolution operator for the 2-DKP,  $\hat{U}^\epsilon$ , has matrix elements  $U_{lm}^\epsilon = U_l^{free} \cdot U_{lm}^{2kick}$  where

$$U_{lm}^{2kick} = \sum_k J_{l-k}(K_\hbar) J_{k-m}(K_\hbar) \exp(-ik^2\hbar_\epsilon/2) \quad (2)$$

where  $J_n$  is the integer Bessel functions of the first kind,  $\hbar_\epsilon = \hbar\epsilon$  is the effective value of Planck’s constant.  $K_\hbar = K_\epsilon/\hbar_\epsilon$  and  $U_{lm}^{free}(\tau_\epsilon) = i^{l-m} \exp(-il^2\tau_\epsilon\hbar_\epsilon/2)$ . To within

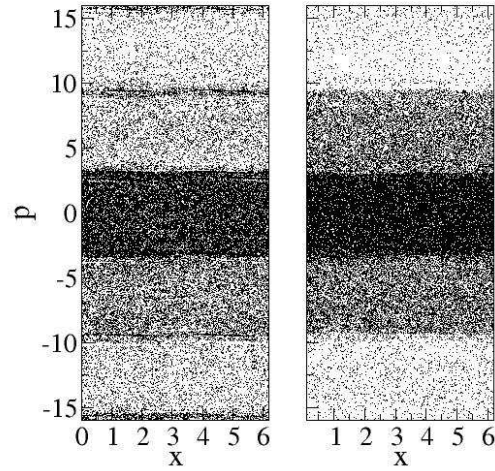


FIG. 1: Comparison of the Poincaré SOS for the 2-DKP and Randomised-Pair DKP. Stochasticity parameter  $K_\epsilon = 0.4$ . **(Left)** 2-DKP:  $\tau_\epsilon = 24$ . A periodic structure of chaotic ‘cells’ separated by thin mixed-phase regions (coinciding with the trapping regions) is apparent. **(Right)** RP-DKP:  $\tau_\epsilon = 10^6$  so impulses between kick pairs are uncorrelated. A similar plot is obtained by taking  $x_{N+2}$  to be a random number. The strength of trapping is largely unchanged, but all remnants of mixed-phase space structures are eliminated. Our key finding here is that the fractional scaling of the *quantum* localization lengths remains unchanged for the RP-DKP.

an unimportant phase, it can be shown that [10]:

$$U_{lm}^{2kick} \simeq J_{l-m} \left( \frac{2K_\epsilon}{\hbar_\epsilon} \cos[l\hbar_\epsilon/2] \right) \quad (3)$$

Eq.3 can be derived most straightforwardly by evaluating the sum in Eq.2 using Poisson summation. The key point is that  $U_{lm}^{2kick}$  is common to all the kicked systems: only  $U_{lm}^{free}(\tau_\epsilon)$  determines whether we investigate the standard DKP ( $\tau_\epsilon = 1$ ), the mixed phase-space 2-DKP ( $1 < \tau_\epsilon \lesssim 100$ ) or the random RP-DKP ( $\tau_\epsilon \rightarrow \infty$ ). Equivalently, we can also obtain the RP-DKP by taking  $U_l^{free} = \exp(-i2\pi\zeta_l)$ , i.e. using random phases for each angular momentum  $l$ . Taking  $\tau_\epsilon = 10^4 - 10^6$  gives the same behavior, provided  $\tau_\epsilon$  is not a rational multiple of  $\pi$ : transport can be strongly affected at such resonances.

Fig.2(a) shows the asymptotic quantum momentum distributions,  $N(p, t \rightarrow \infty)$ , obtained from an initial state  $\psi(t=0) \sim \delta(p - p_0)$  for  $p_0 = 0$ , in regimes analogous to Fig.1. The dashed line corresponds to a momentum distribution obtained for the mixed phase-space 2-DKP while the solid line represents the equivalent result obtained using random phases in  $U_l^{free}$ . One sees that both the mixed phase-space 2-DKP and the random map (RP-DKP) distributions are very similar, with a distinctive ‘staircase’ structure.

Fig.2(b) shows the staircases obtained for  $K_\epsilon = 0.4$ ,  $\hbar_\epsilon = 1/25, 1/250$  and  $\hbar_\epsilon = 1/2500$  for the 2-DKP. We have rescaled the momentum distributions  $N(p)$  using

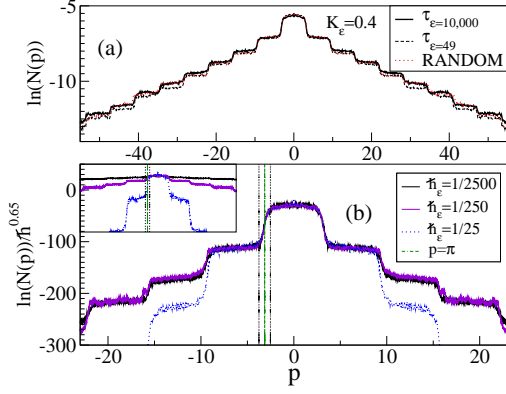


FIG. 2: **(a)** Shows that the quantum momentum distributions for the mixed phase-space double kicked atoms (2-DKP) are similar to those of the RP-DKP, for which the phases between kick pairs are random numbers. The staircase structure and ‘heights’ of the steps are comparable.  $K_\epsilon = 0.4$  and  $\hbar_\epsilon = 1/500$  in every case. **(b)** Shows the fractional scaling for the 2-DKP.  $K_\epsilon = 0.4$  and  $\tau_\epsilon = 49$ . The  $\hbar_\epsilon^{2/3}$  rescaling of the momentum distributions shows that the first step scales near-perfectly in the range from  $\hbar_\epsilon = 1/2500$  to  $1/25$ ; i.e. the ‘local’ localization length in the trapping region scales over this entire  $\hbar_\epsilon$  range. The global localization length (the envelope of the whole distribution) shows this fractional  $\hbar_\epsilon$  scaling holds only for the smaller  $\hbar_\epsilon = 1/2500$  and  $\hbar_\epsilon = 1/250$  but not for  $\hbar_\epsilon = 1/25$ . Vertical lines indicate width and centre ( $p = \pi$ ) of the first trapping region. The inset shows the same curves without the  $\hbar_\epsilon^{2/3}$  scaling.

the ‘local’ scaling exponent estimated in Fig.3 for  $K_\epsilon = 0.4$  which yielded  $\sigma \approx 0.65$ . We plot  $\ln(N(p))\hbar_\epsilon^{-0.65}$ , shifted by an appropriate constant. The figure shows that the shape and magnitude of the distribution around the first trapping region re-scales perfectly with  $\hbar_\epsilon$ .  $L_{loc}$  is the slope on the first step. The height of the steps ( $2d$  in the notation of [10]) scales fractionally with  $\hbar_\epsilon$ , while the width  $w$  (momentum width between the dashed vertical lines) is independent of  $\hbar_\epsilon$ : in scaled momentum units  $w \sim 2\pi/6$ . Thus we take  $L_{loc} \approx w/2d$ , i.e. for the scaling,  $L_{loc} \sim (2d)^{-1}$ .

The longer-ranged localization length  $L$ , characterizing the envelope of the full staircase, scales well in the smaller  $\hbar_\epsilon$  range  $\hbar_\epsilon \lesssim 1/250$  but we note that the  $\hbar_\epsilon = 1/25$  staircase does not scale at long-range.

In Fig.3 we investigate the  $\hbar_\epsilon$  scaling exponent itself. For staircases where  $\hbar_\epsilon$  is sufficiently small,  $\ln(N(p)) \approx \text{const}$  outside the ‘steps’ in the trapping regions. Then, only the step heights depend on  $\hbar_\epsilon$ . We can restrict ourselves to a study of the parameter  $2d$  since it has the same  $\hbar_\epsilon$  scaling as  $L_{loc}$ . The midpoint of the  $n$ -th step is at  $p_{1/2}^{(n)} = 2(n-1)\pi/\epsilon$  for  $n \neq 1$ ; for  $n = 1$ , we take  $p_{1/2}^{(1)} = \pi/(2\epsilon)$ . For the  $n$ -th step we measure

$$2d(n) = \langle \ln(N(p_{1/2}^{(n)})) \rangle - \langle \ln(N(p_{1/2}^{(n+1)})) \rangle \quad (4)$$

where the average is taken over a small momentum in-

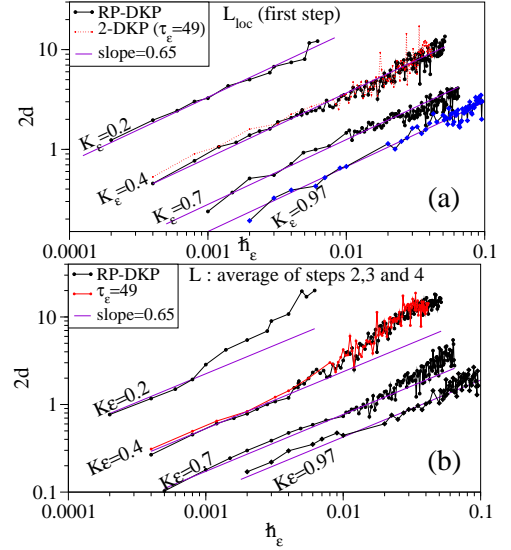


FIG. 3: **(a)** Fractional scaling of the  $L_{loc}$  (the localization length at the first step: note that  $L_{loc} \sim (2d)^{-1}$ ). It shows the fractional  $2d \sim \hbar_\epsilon^{2/3}$  scaling holds over the full  $\hbar_\epsilon$  range. Straight lines indicate slope 0.65. The  $\approx 2/3$  scaling holds even for  $K_\epsilon = 0.97 \approx K_c$ , the parameter for criticality in the Standard Map: the only difference is that here  $\tau_\epsilon \rightarrow \infty$  (RP-DKP) instead of  $\tau_\epsilon = 1$  (Standard Map). **(b)** As for (a) but shows the average of steps 2 to 4, showing that the  $L \sim \hbar_\epsilon^{-2/3}$  global scaling persists only for the smaller  $\hbar_\epsilon$  values.

terval around  $p_{1/2}^{(n)}$ . This procedure is easily automated, allowing a very fine-grid of  $\hbar_\epsilon$  values, so we can examine fluctuations in behavior.

Fig.3(a) compares the  $\hbar_\epsilon$  scaling of  $2d(1)$  for the 2-DKP and the RP-DKP, while Fig.3(b) shows the average of  $2d$  for steps  $n=2$  to 4. We take the behavior of the first step to indicate the local localization length and of steps 2 to 4 to indicate the properties of the long-ranged scaling. All the plots, whether 2-DKP or RP-DKP, show a slope  $\sigma \approx 0.65$  for small  $\hbar_\epsilon$ . For the upper ranges of  $\hbar_\epsilon$ , the slope (for  $L$  only) increases significantly. These results are quite consistent with the slightly higher estimate  $\sigma \approx 0.75$  found in [10]: there, an average of the first few steps was obtained, including a few  $\hbar_\epsilon$  values in the range where the deviation from  $\sigma \approx 2/3$  begins.

We note that the trapping regions and the Standard Map golden cantori regions occupy similar regions of phase-space: the golden tori occur at winding number  $p_0/2\pi \approx 0.618$  and  $p_0/2\pi \approx (1 - 0.618)$ . The trapping occurs for  $p_0/2\pi \approx 0.5$  (e.g. momentum  $p \approx \pi$ ), exactly midway between these. In Fig.(4) we show the well-known plot of Geisel et al (Fig.2(b) in [6]) reproduced in quantum chaos textbooks [11]. In that study, an initial state  $\psi(t=0) \sim \delta(p-p_0)$  was evolved for critical  $K_c \approx 0.9716$  to study transport through the golden cantori. Notably, that study used precisely  $p_0 = 3.2 \approx \pi$ : the initial state was centred in the trapping region. We

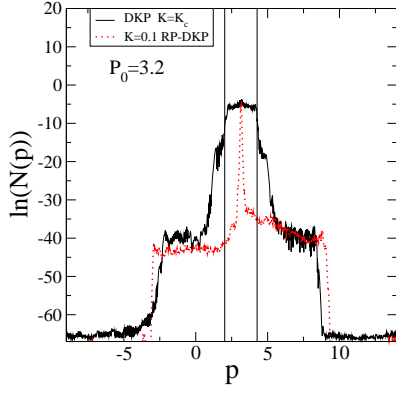


FIG. 4: Figure shows that the RP-DKP trapping regions coexist with the phase space regions which contain the two ‘golden ratio’ tori of the DKP (Standard Map); nevertheless, destroying the cantori in the RP-DKP with random phases does not eliminate fractional scaling. (Bold solid lines) DKP at critical  $K_c \approx 0.97$ ; the plot is similar to Fig.2b of Geisel et al 1986 [6] which yielded  $L_{loc} \sim \hbar^{+2/3}$ . Vertical lines indicate ‘golden’ tori. Graph was obtained by setting  $K_\epsilon = K_c = 0.97$ ,  $\tau_\epsilon = 1$ ,  $\hbar_\epsilon = 0.01$ . (Dotted line) the RP-DKP distribution is shown for a kick strength  $K_\epsilon = 0.1$ , sufficiently small that the amplitude ‘drops’ are comparable in magnitude to the DKP (but without the golden cantori).

compare a RP-DKP result also with  $p_0 = 3.2 \approx \pi$  but destroying all the KAM structures including cantori by taking  $\tau_\epsilon \rightarrow \infty$  but otherwise running exactly the same numerical code (We take the same  $\hbar = 1/100$  but  $K = 0.1$  for the RP-DKP to keep diffusion rates comparable to the DKP). Since  $\epsilon$  is our unit of time in both systems, we can drop the  $\epsilon$  subscripts on  $\hbar$  and  $K$ .

We now analyze the cause of the  $L \sim \hbar^{-2/3}$  scaling of the RP-DKP. We consider the trapping regions  $\delta p = (p - p_0)$  centered at  $p_0 = l_0 \hbar = (2n + 1)\pi$ . At the centers of these regions the argument of the Bessel function in Eq.3 vanishes. Near these points it is of appreciable size up until when its argument  $x = \frac{2K}{\hbar} \cos[l\hbar/2]$  is of the order of the index; i.e. when  $x \lesssim |l - m|$ . If also  $|l - m| \gg 1$ , the asymptotic approximation

$$U_{lm}^{2kick} \sim J_{l-m}(x) \sim \frac{2^{1/3}}{|l - m|^{1/3}} Ai(-2^{1/3}z), \quad (5)$$

with  $x = |l - m| + \frac{z}{|l - m|^{1/3}}$ , holds.  $\delta p$  is small, as we are near the center of a bottleneck, so this implies we are in the semiclassical,  $\hbar \rightarrow 0$ , regime. Heuristically, the transition probability corresponding to a small change in momentum  $\Delta p$  is  $|U_{lm}^{2kick}|^2$ , which is proportional to  $|l - m|^{-2/3} = \frac{\hbar^{2/3}}{\Delta p^{2/3}}$  (where  $\Delta p = |l - m|\hbar$ ). The effect of  $U_{lm}^{free}$  is to randomize the phases. The trapping regions act as bottlenecks for transport. On scales larger than  $\Delta p$ , considered fixed, diffusion takes place:  $p^2 \sim Dt$ , where the local diffusion coefficient  $D$  is proportional to  $|U_{lm}^{2kick}|^2$  and therefore to  $\hbar^{2/3}$ . Assuming that the evolution operator is a band-matrix with constant width (as

is the situation for the ordinary Kicked-Rotor), the local localization length satisfies [4, 12]  $L_{local} \sim \frac{D}{\hbar}$ , implying  $L_{local} \sim \hbar^{-1/3}$ . In our case, the width of the contributing region, as implied by the scaling of the argument of the Airy function in Eq. (6), is of the order  $|l - m|^{1/3} = \frac{\Delta p^{1/3}}{\hbar^{1/3}}$ . This should multiply the expressions for  $D$  and  $L_{local}$ . The resulting localization length therefore satisfies  $L \sim \hbar^{-2/3}$ . The condition for the validity of the asymptotic properties of the Bessel function and for the momentum to be in a bottleneck region is  $1 \gg \cos[l\hbar/2] \gg \frac{\hbar}{2K}$ .

We recall that this structure of  $U_{lm}^{2kick}$  is common to both the quantum DKP as well as RP-DKP; and Fig.4 shows that the fractional scaling, is observed over similar phase-space regions. One may safely conclude from the analysis here that the behaviour of the generic RP-DKP follows only from the semiclassical dynamics in the bottleneck regions: it is the hallmark of the scaling of an Airy function rather than of the fractal scaling near golden cantori. However, for the DKP, the additional presence of large stable islands bordering the regions where  $\hbar^{2/3}$  is observed (which occur when  $\tau_\epsilon \approx 1$ ) make the quantum-classical interplay less transparent. In this case too, Airy functions and  $\hbar^{2/3}$  factors occur naturally in the semiclassical quantization of torus states [13]. A much more detailed study than the one undertaken here is required to conclusively establish whether the semiclassical dynamics is also the dominant mechanism in the quantum DKP, but we suggest that cantori do not represent the only possible source for  $\hbar^{\pm 2/3}$  scaling behavior.

The authors thank C.Creffield and A. M. García-García for helpful discussions. J.W. acknowledges support from Defence Science and Technology Agency (DSTA) of Singapore under agreement of POD0613356.

---

\* t.monteiro@ucl.ac.uk

- [1] E. Ott, ‘Chaos in Dynamical Systems’, Cambridge University Press (1993).
- [2] L.E. Reichl ‘The transition to chaos’.2nd Ed.Springer, New York, (2004); H-J. Stockman, ‘Quantum Chaos’,C.U.P. (1999).
- [3] G. Casati, B.V. Chirikov, F.M. Izraelev, J. Ford, *Lecture Notes in Physics* Vol. 93 (Springer, Berlin, 1979), p. 334
- [4] S. Fishman, D.R. Grempel, R.E. Prange, Phys. Rev. Lett. **49**, 509 (1982); D.L. Shepelyansky, Phys. Rev. Lett. **56**, 677 (1986).
- [5] F.L. Moore, J.C. Robinson, C.F. Bharucha, B. Sundaram, M.G. Raizen, Phys. Rev. Lett. **75**, 4598 (1995); H. Ammann, R. Gray, I. Shvarchuck, N. Christensen, Phys. Rev. Lett. **80**, 4111 (1998); M.K. Oberthaler, R.M. Godun, M.B. d’Arcy, G.S. Summy, K. Burnett, Phys. Rev. Lett. **83**, 4447 (1999); P. Szriftgiser, J. Ringot, D. Delande, J.C. Garreau, Phys. Rev. Lett. **89**, 224101 (2002); G.J. Duffy, S. Parkins, T. Muller, M. Sadgrove, R. Leonhardt, A.C. Wilson, Phys. Rev. E **70**, 056206

- (2004); P.H. Jones, M. Goonasekera, D.R. Meacher, T. Jonckheere, T.S. Monteiro Phys. Rev. Lett. **98**, 073002 (2007).
- [6] T. Geisel, G. Radons and J. Rubner Phys. Rev. Lett. **57**, 2883 (1986); G. Radons and R. Prange, Phys. Rev. Lett. **61**, 1691 (1988).
- [7] N.T. Maitra and E.J. Heller, Phys. Rev. E. **61**, 3620 (2000).
- [8] S. Fishman, D.R. Grempel, R.E. Prange, Phys. Rev. A **36**, 289 (1987).
- [9] P.H. Jones, M.M.A. Stocklin, G. Hur, T.S. Monteiro, Phys. Rev. Lett. **93**, 223002 (2004).
- [10] C.E. Creffield, G. Hur, T.S. Monteiro, Phys. Rev. Lett. **96**, 024103 (2006) C.E. Creffield, S. Fishman, T.S. Monteiro, Phys. Rev. E. **73**, 066202 (2006).
- [11] See Stockmann p.12 or Reichl p.443 (texts in ref[2]).
- [12] D.L. Shepelyansky, Phys. Rev. Lett. **56**, 677 (1986); Physica **D28**, 103 (1987).
- [13] M.V. Berry, Phil. Trans. Roy. Soc. **287** 237 (1977).